Energy-loss straggling with higher-order effects and electron correlations taken into account

V. A. Khodyrev *

Skobeltsyn Institute of Nuclear Physics, Moscow State University, Moscow 119899, Russia

(Received 13 March 2019; revised manuscript received 14 August 2019; published 23 September 2019)

The approach suggested previously to treat the mean energy loss of charged projectiles in terms of induced currents is extended to describe the energy-loss straggling. It has been shown that, provided the perturbed wave function of electrons is known, the phenomenon can be represented in a form of distributions of densities of energy and energy squared within the target volume. These distributions satisfy respective continuity equations with the source terms defining the local deposition of energy and energy squared. The approach is applied to treat the canonical phenomenon, the stopping in a uniform electron gas, and provides a possibility to account for the spatial correlation of electrons. Two types of approximations for the perturbed state of electrons are considered, the impulse and continuum distorted-wave approximations. Together with the effect of electron correlations, these nonperturbative approaches permit one to evaluate the higher-order correction over the projectile charge. The origin of this correction is similar to the origin of Barkas correction in the stopping power; it can be argued also that there is no place in straggling for the Bloch correction. These properties, i.e., nonlinear electron response and electron correlations, can result in significant effects, both capable of changing dramatically the straggling at small projectile energies. However, in the case of positively charged projectiles, the two effects mainly compensate for one another. For negatively charged projectiles, due to the impossibility of close approaches of the collision partners, both effects are effectively smeared out.

DOI: 10.1103/PhysRevA.100.032711

I. INTRODUCTION

Straggling of energy loss of swift charged particles is mainly due to violent close collisions with electrons. For the energy spread Ω of a charged particle penetrating a gas of noninteracting electrons, Bohr [1] gave the simple expression

$$\Omega^2 = \langle E^2 \rangle - \langle E \rangle^2 = \Omega_B^2 = 4\pi Z_1^2 e^4 n \Delta R, \qquad (1)$$

where $Z_1 e$ is the charge of the projectile, n is the electron gas density, and ΔR is the thickness of the traversed layer of electron gas. The electrons are considered herein as being initially at rest, and, due to the coincidence of the scattering cross sections, the result (1) is valid in both classical and quantum mechanics.

More effort is required to account for the states of electrons in real matter. Considering the same case of a uniform electron gas, one has to estimate the effect of initial motion of electrons and of interelectron interaction. Both effects are accounted for in Lindhard's treatment of uniform gas of interacting electrons with a Fermi distribution of their momenta where the response of electrons to external perturbation is described in the random-phase approximation (RPA) [2]. As expected, the main corrections to Bohr's result appear at small projectile velocities when the gas has a chance to react to the change of state of a separate electron [3]. Chu [4] used these results to describe straggling in the case of an atomic target: The RPA results were averaged over the distribution of electron density in the atomic shell.

Another important ingredient of straggling theory is the statistics of collisions with electrons. The Poisson distribution of the number of collisions with a certain impact parameter and its quantum-mechanical equivalent were assumed in the developments described above. In reality, however, electron density is nonuniform since electrons are clustered in atomic shells. On an even smaller scale, the positions of electrons are correlated due to their Coulomb repulsion and quantum exchange, the phenomenon commonly referred to as electron correlation. These two effects can be considered separately as follows from the rule of variance decomposition [5].

Sigmund [6] considered the effect of the atomic structure of the stopping medium. For this goal, the projectile-atom collisions can be considered as elementary events with the mean energy loss depending on the impact parameter. Thus, one encounters here the only essential problem: In the case of a molecular gas or solid target the Poisson statistics of projectile-atom collisions is modified due to the correlations of atom positions.

The main topic of this paper is the effect of electron correlations. As a basis for this consideration, the model of uniform electron gas should be appropriately developed and then Chu's model can be accordingly improved. It is easy to show that only pair correlations are essential to determine the second moment of energy-loss distribution. Meshakin [7] approached this problem by applying the impulse approximation to treat collisions with each electron of the pair. However, it seems hardly appropriate to consider these collisions as a superposition of two finished collisions; the correlation length could be of the same order as the range of projectile-electron interaction. This is illustrated in Sec. III, where the impulse approximation is applied in its standard form [8].

*khodyrev@anna19.sinp.msu.ru

Recently [9], *ab initio* numerical calculations of the energy loss and energy-loss straggling were fulfilled for the simplest correlated system, the He atom. The results show that the straggling is sensitive to the correlation in simultaneous excitations of two electrons. However, the primary effect in this case is not the correlation of electron locations but the shake-up processes: In the two-electron system, the eigenstates of an electron are modified when the second electron is excited.

For a uniform electron gas, the simplest way to estimate the effect of electron correlations is replacement of the statistics of independent collisions in Bohr's classical model by statistics with a different distribution of distances between consecutive collisions. Such a generalization of statistics is treated by the renewal theory [10]. In a quantum-mechanical description, one has to consider from the outset the target electrons as a multiparticle system whose properties are presented by a nontrivial density matrix.

In this paper, the problem is treated using the approach proposed in Ref. [11], where energy deposition in the stopping medium is described by a continuity equation for the energy density distribution. In the treatment of stopping in an electron gas, this nonperturbative method has demonstrated its efficiency, showing in particular the origin of the higher-order corrections over the projectile charge. The approach also accounts for the screening of the projectile field due to the electron gas polarization [12]. In Sec. II this method is extended to develop an analogous description of the deposition of energy squared. The possible use of the impulse approximation (IA) for treatment of the straggling is discussed in Sec. III. In Sec. IV the current density approach is applied using the continuum distorted-wave (CDW) approximation for the electron wave function perturbed by the projectile field. The results of numerical calculations are shown in Sec. V. A summary is given in Sec. VI.

Atomic units are used throughout unless stated differently.

II. CONTINUITY EQUATIONS

A detailed picture of energy deposition in the stopping medium can be presented by the evolution of the energy density and its flux in the volume around the moving projectile. Analogously, the mean square of energy of electrons $\langle E^2\rangle$ can be determined by integration of the density of energy squared. Let us define the interesting densities in the configuration space $\mathbb{R} = \{\boldsymbol{r}_1, \ldots, \boldsymbol{r}_N\}$ of all N electrons as

$$\rho(\mathbb{R}, t) = \Psi^*\Psi, \tag{2a}$$

$$\rho_E(\mathbb{R}, t) = \tfrac{1}{2}(\Psi^* \cdot \mathcal{H}_0\Psi + \mathcal{H}_0\Psi^* \cdot \Psi), \tag{2b}$$

$$\rho_{E^2}(\mathbb{R}, t) = \mathcal{H}_0\Psi^* \cdot \mathcal{H}_0\Psi, \tag{2c}$$

where $\Psi(\mathbb{R}, t)$ is the wave function of electrons and

$$\mathcal{H}_0 = \mathcal{T} + V_{ee} + V_{en} \tag{3}$$

is the unperturbed Hamiltonian with

$$\mathcal{T} = \sum_j \mathcal{T}_j = \sum_j -\frac{\Delta_j}{2} \tag{4}$$

as the kinetic energy operator, $V_{ee}(\mathbb{R})$ the interelectron interaction, and $V_{en}(\mathbb{R})$ the potential energy of the interaction of electrons with the nuclei of atoms of the stopping medium. The wave function Ψ is asymmetric over electron permutations; the spin coordinates insignificant in the present task are omitted. So defined ρ_E and ρ_{E^2} are real valued and their integration over space gives the actual expectations of the self-energy of electrons and its square.

Continuity equations for the densities ρ_E and ρ_{E^2} can be derived by a procedure analogous to that used in the derivation of equation for ρ [13]. The evolution of $\Psi(\mathbb{R}, t)$ in (2) is determined by the Schrödinger equation

$$i\frac{\partial\Psi}{\partial t} = (\mathcal{H}_0 + U)\Psi, \tag{5}$$

where

$$\mathcal{U} = \sum_i V(\boldsymbol{r}_i - \boldsymbol{R}) = \sum_i -\frac{Z_1}{|\boldsymbol{r}_i - \boldsymbol{R}|} \tag{6}$$

is the potential of electron interaction with the projectile at its current position $\boldsymbol{R}(t)$. Then, in the resulting expressions for the time derivatives of densities (2), the coordinate derivatives of the kinetic energy operator $\mathcal{T}$ can be rearranged, transforming the equations to

$$\frac{\partial\rho}{dt} = -\nabla_i \boldsymbol{j}_i, \tag{7a}$$

$$\frac{\partial\rho_E}{dt} = -\nabla_i \boldsymbol{j}_{E,i} + \boldsymbol{\mathcal{E}}_i \boldsymbol{j}_i, \tag{7b}$$

$$\frac{\partial\rho_{E^2}}{dt} = -\nabla_i \boldsymbol{j}_{E^2,i} + 2\,\boldsymbol{\mathcal{E}}_i \boldsymbol{j}_{E,i}, \tag{7c}$$

where $\boldsymbol{\mathcal{E}}_i = -\nabla_i V(\boldsymbol{r}_i - \boldsymbol{R})$ is the projectile electric force acting on the ith electron (summation over repeating indices is assumed here and later on). The current densities related to the densities ρ, ρ_E, and ρ_{E^2} are defined as

$$\boldsymbol{j}_i(\mathbb{R}, t) = \frac{1}{2i}\Psi^* \overleftrightarrow{\partial_i} \Psi, \tag{8a}$$

$$\boldsymbol{j}_{E,i}(\mathbb{R}, t) = \frac{1}{4i}(\Psi^* \overleftrightarrow{\partial_i} \mathcal{H}_0\Psi + \mathcal{H}_0\Psi^* \overleftrightarrow{\partial_i} \Psi), \tag{8b}$$

$$\boldsymbol{j}_{E^2,i}(\mathbb{R}, t) = \frac{1}{2i}\mathcal{H}_0\Psi^* \overleftrightarrow{\partial_i} \mathcal{H}_0\Psi - \boldsymbol{\mathcal{E}}_i \frac{\partial\rho}{\partial t}, \tag{8c}$$

where $A \overleftrightarrow{\partial_i} B = A \cdot \nabla_i B - \nabla_i A \cdot B$.

In order to interpret the source terms in the continuity equations (7b) and (7c) as describing the local deposition of energy and energy squared, one has to ensure that the integrals of divergence of the fluxes $\boldsymbol{j}_E$ and $\boldsymbol{j}_{E^2}$ over all space are vanishing. This is equivalent to the requirement that there are no runoffs at the points of Coulomb singularities of the potentials. It can be shown that, due to the Kato cusp condition [14] for the wave function $\Psi(\mathbb{R}, t)$, this requirement is fulfilled. Notice that, in this respect, the presence of the term on the right-hand side of (8c) which explicitly depends on the projectile-electron interaction $\boldsymbol{\mathcal{E}}_i$ is of key importance. Although this term only negligibly contributes to the flux at large distances and vanishes in the classical limit (an additional factor $\hbar^2$ is omitted in using atomic units), it is significant as compensating a nonzero runoff at $\boldsymbol{r}_i = \boldsymbol{R}(t)$ due to the first term.

Thus, the time variation of the mean value $\langle E^2\rangle$, determining the mean square of energy loss of the projectile, is given by

the integral over all the volume of the source term $2\mathcal{E}_i \boldsymbol{j}_{E,i}$ in Eq. (7c). Notice that, like all other terms in Eqs. (7), this one also has the form of the corresponding classical expression. The straggling Ω^2 is determined in terms of densities (2) and current densities (8) as

$$\frac{d\Omega^2}{dt} = \frac{d\langle E^2\rangle}{dt} - 2\langle E\rangle \frac{d\langle E\rangle}{dt}, \tag{9}$$

where

$$\langle E\rangle = \int d\mathbb{R}\, \rho_E(\mathbb{R}, t), \tag{10}$$

$$\frac{d\langle E\rangle}{dt} = \int d\mathbb{R}\, \boldsymbol{\mathcal{E}}(\boldsymbol{r}_i, t)\boldsymbol{j}_i(\mathbb{R}, t), \tag{11}$$

$$\frac{d\langle E^2\rangle}{dt} = 2\int d\mathbb{R}\, \boldsymbol{\mathcal{E}}(\boldsymbol{r}_i, t)\boldsymbol{j}_{E,i}(\mathbb{R}, t). \tag{12}$$

If the wave function $\Psi(\mathbb{R}, t)$ is known, the method described above enables calculation of both the mean energy loss and the energy-loss straggling. In the two following sections, the impulse and CDW approximations for the wave function of a uniform electron gas perturbed by the projectile field are used to describe the straggling of energy loss.

III. IMPULSE APPROXIMATION

In this approximation, all internal interactions in the target atom are disregarded during the collision, $\mathcal{H}_0 \approx \mathcal{T}$. The respective form of the perturbed wave function Ψ is obtained [8] by a proper modification of its representation in the momentum space

$$\Psi(\mathbb{R}, t) = \sum_{\mathbb{K}} f_{\mathbb{K}} \exp(i\mathbb{K}\mathbb{R}), \tag{13}$$

where $\mathbb{K} = \{\boldsymbol{k}_1, \ldots, \boldsymbol{k}_N\}$ is the set of momenta $\boldsymbol{k}_i$ of all electrons. Each plane wave $e^{i\boldsymbol{k}_i\boldsymbol{r}_i}$ here is replaced by the wave of scattering in the projectile frame $\psi^{(+)}$,

$$e^{i\boldsymbol{k}_i\boldsymbol{r}_i} \to e^{i\boldsymbol{v}\boldsymbol{r}_i} e^{i\boldsymbol{k}_i\boldsymbol{R}} \psi^{(+)}_{\boldsymbol{k}_i-\boldsymbol{v}}(\boldsymbol{r}_i - \boldsymbol{R}), \tag{14}$$

where $\boldsymbol{v}$ is velocity of the projectile assumed as moving along a straight-line trajectory. The exponential factors on the right-hand side of (14) appear as a result of the transformation to the laboratory frame with the coordinate origin at $\boldsymbol{R}$.

Although the results obtained will be the same, it is convenient to follow here a simpler procedure than that described in the preceding section. The quantities on the right-hand side of (9) can be determined using the equations

$$\langle E\rangle = \langle\Psi|\mathcal{H}_0|\Psi\rangle \approx \langle\Psi|\mathcal{T}|\Psi\rangle, \tag{15}$$

$$\frac{d\langle E\rangle}{dt} = \frac{1}{i}\langle\Psi|[\mathcal{H}_0, \mathcal{H}]|\Psi\rangle \approx \frac{1}{i}\langle\Psi|[\mathcal{T}, \mathcal{U}]|\Psi\rangle, \tag{16}$$

$$\frac{d\langle E^2\rangle}{dt} = \frac{1}{i}\langle\Psi|[\mathcal{H}_0^2, \mathcal{H}]|\Psi\rangle \approx \frac{1}{i}\langle\Psi|[\mathcal{T}^2, \mathcal{U}]|\Psi\rangle. \tag{17}$$

Insertion of the wave function (13) with distortion (14) into (15) results in the equation

$$\langle E\rangle \approx \langle\Psi|\sum_i \mathcal{T}_i|\Psi\rangle = \sum_i \sum_{\mathbb{K},\mathbb{K}'} f^*_{\mathbb{K}'} f_{\mathbb{K}} e^{i(\boldsymbol{k}_i - \boldsymbol{k}'_i)\boldsymbol{R}} \times (\boldsymbol{k}'_i - \boldsymbol{v}|e^{-\boldsymbol{v}\boldsymbol{r}_i}\mathcal{T}_i e^{\boldsymbol{v}\boldsymbol{r}_i}|\boldsymbol{k}_i - \boldsymbol{v}). \tag{18}$$

Here $|\boldsymbol{k}_i - \boldsymbol{v})$ is the state of scattering with the wave function $\psi^{(+)}_{\boldsymbol{k}_i-\boldsymbol{v}}(\boldsymbol{r}_i - \boldsymbol{R})$ in (14). The addition of the sum of intermediate momentum states, the operators $|\mathbf{q}_i\rangle\langle\mathbf{q}_i|$, ahead of $\mathcal{T}_i$ puts the matrix element in (18) in the form

$$\sum_{\boldsymbol{q}_i} \frac{q_i^2}{2}(\boldsymbol{k}'_i - \boldsymbol{v}|\mathbf{q}_i - \boldsymbol{v}\rangle\langle\mathbf{q}_i - \boldsymbol{v}|\boldsymbol{k}_i - \boldsymbol{v}). \tag{19}$$

Analogously, Eq. (16) is transformed to

$$\frac{d\langle E\rangle}{dt} \approx 2\,\mathrm{Re}\sum_i \sum_{\mathbb{K},\mathbb{K}'} f^*_{\mathbb{K}'} f_{\mathbb{K}} e^{i(\boldsymbol{k}_i - \boldsymbol{k}'_i)\boldsymbol{R}} \times \frac{1}{i}\sum_{\boldsymbol{q}_i}\frac{q_i^2}{2}(\boldsymbol{k}'_i - \boldsymbol{v}|\mathbf{q}_i - \boldsymbol{v}\rangle\langle\mathbf{q}_i - \boldsymbol{v}|V|\boldsymbol{k}_i - \boldsymbol{v}). \tag{20}$$

Averaging of the exponential factor over $\boldsymbol{R}$ results in the appearance of the delta function $\delta(\boldsymbol{k}_i - \boldsymbol{k}'_i)$. Hence, for each i, the sum over $\mathbb{K}$ and $\mathbb{K}'$ converges to the sum over $\boldsymbol{k}_i$ of diagonal elements of the one-electron density matrix $f^*_{\boldsymbol{k}_i} f_{\boldsymbol{k}_i}$. Also, the summation over i is trivial: All electrons give identical contributions. Further, we have the relation [13]

$$\langle\mathbf{q} - \boldsymbol{v}|V|\boldsymbol{k} - \boldsymbol{v}) = -2\pi A(\boldsymbol{k} - \boldsymbol{v}, \boldsymbol{q} - \boldsymbol{v}), \tag{21}$$

where $A(\boldsymbol{k} - \boldsymbol{v}, \boldsymbol{q} - \boldsymbol{v})$ is the amplitude of scattering from the state $|\boldsymbol{k} - \boldsymbol{v}\rangle$ to $|\boldsymbol{q} - \boldsymbol{v}\rangle$, and the momentum representation of the scattering state $|\boldsymbol{k} - \boldsymbol{v})$ is given as

$$\langle\mathbf{q} - \boldsymbol{v}|\boldsymbol{k} - \boldsymbol{v}) = \delta(\mathbf{q} - \mathbf{k}) + \frac{1}{2\pi^2}\frac{A(\boldsymbol{k} - \boldsymbol{v}, \boldsymbol{q} - \boldsymbol{v})}{\frac{(\boldsymbol{q}-\boldsymbol{v})^2}{2} - \frac{(\boldsymbol{k}-\boldsymbol{v})^2}{2} - io}. \tag{22}$$

The presence of the delta function $\delta(\mathbf{q} - \mathbf{k})$ here results in the appearance of a combination of two terms in (20) with the forward scattering amplitude $A(\boldsymbol{k} - \boldsymbol{v}, \boldsymbol{k} - \boldsymbol{v})$ which are suited for application of the optical theorem.

With all this taken together, Eq. (20) acquires the form

$$\frac{d\langle E\rangle}{dt} = n\int d\boldsymbol{k}|f_k|^2 \int d\boldsymbol{q}\left(\frac{q^2}{2} - \frac{k^2}{2}\right)|A(\boldsymbol{q} - \boldsymbol{v}, \boldsymbol{k} - \boldsymbol{v})|^2 \times \delta\left(\frac{(\boldsymbol{q} - \boldsymbol{v})^2}{2} - \frac{(\boldsymbol{k} - \boldsymbol{v})^2}{2}\right), \tag{23}$$

where n is the electron density. In the case of electrons being initially at rest, $\boldsymbol{k} = 0$, this is nothing but the familiar representation of energy loss through the transport cross section.

Relying more on the CDW method considered in Sec. IV, I do not treat here the straggling in detail. I mention only the main differences from the mean energy loss and compare this approach with the approach used in [7]. The difference between (16) and (17) is that the operator $\mathcal{T}^2$ contains not only the single-electron terms $\mathcal{T}_i^2$, but also the two-electron terms $\mathcal{T}_i\mathcal{T}_j$. For the former, the above procedure results in replacement of the terms $q^2/2$ and $k^2/2$ in expression (23) by their squares. This result is readily associated with Bohr's picture of the phenomenon, and, in the case of purely Coulomb interaction, the straggling is given again by the formula (1).

For collisions with two electrons, the equation for $d\langle\mathcal{T}_i\mathcal{T}_j\rangle/dt$ with $i \neq j$ has the form of Eq. (20) with respective modifications on its right-hand side. First, instead of two states of the ith electron with the momenta $\boldsymbol{k}_i$ and $\boldsymbol{k}'_i$ we have now

two pairs of states with momenta $\boldsymbol{k}_i$ and $\boldsymbol{k}_j$ and momenta $\boldsymbol{k}'_i$ and $\boldsymbol{k}'_j$ and also two final states with momenta $\boldsymbol{q}_i$ and $\boldsymbol{q}_j$. In turn, this results in the necessity to consider the two-electron density matrix $f^*_{\boldsymbol{k}'_i\boldsymbol{k}'_j} f_{\boldsymbol{k}_i\boldsymbol{k}_j}$ while the averaging over $\boldsymbol{R}$ establishes a less restrictive relation of the momenta: $\boldsymbol{k}'_i + \boldsymbol{k}'_j = \boldsymbol{k}_i + \boldsymbol{k}_j$. Finally, instead of the last factor in the integrand in (20) we will have

$$(\boldsymbol{k}'_j - \boldsymbol{v}|\mathbf{q}_j - \boldsymbol{v}\rangle\langle\mathbf{q}_j - \boldsymbol{v}|\boldsymbol{k}_j - \boldsymbol{v})(\boldsymbol{k}'_i - \boldsymbol{v}|\mathbf{q}_i - \boldsymbol{v}\rangle \times \langle\mathbf{q}_i - \boldsymbol{v}|V|\boldsymbol{k}_i - \boldsymbol{v}). \tag{24}$$

With this expression, where the entering matrix elements are determined by (21) and (22), the contribution of collisions with two electrons can be presented by a set of Feynman diagrams. Their number suggests that such calculations would require considerable effort. A simpler expression is used in [7], where in fact the product of four respective scattering amplitudes is used instead of (24). This is, however, just one diagram; the contribution of others is left uncertain.

Finally, it is easy to verify that in the absence of correlations $f_{\boldsymbol{k}_i\boldsymbol{k}_j} = f_{\boldsymbol{k}_i} f_{\boldsymbol{k}_j}$, the contribution of collisions with two different electrons in $\langle E^2\rangle$ is exactly compensated when the variation of the square of the mean energy is subtracted [Eq. (9)]. So, as expected, the principal property of statistics of classical independent collisions is exactly reproduced.

IV. DISTORTED-WAVE APPROACH

In this approach, the wave function Ψ is approximated as [15]

$$\Psi = \mathcal{D}\Psi_0, \tag{25}$$

where Ψ_0 is the wave function of the unperturbed ground state of electrons and the factor $\mathcal{D}(\mathbb{R}, t)$ accounts for the distortion due to the projectile field $\mathcal{U}$. If this factor is chosen so that it satisfies the equation

$$i\frac{\partial}{\partial t}\mathcal{D} = (\mathcal{T} + \mathcal{U})\mathcal{D}, \tag{26}$$

the wave function Ψ [Eq. (25)] satisfies the wave equation with the residue $\nabla_i\mathcal{D}\cdot\nabla_i\Psi_0$. It is argued that, at sufficiently large energy of the projectile, this term can be disregarded.

In this approximation,

$$\mathcal{H}_0\Psi = \mathcal{T}\mathcal{D}\cdot\Psi_0 + E_0\Psi, \tag{27}$$

where E_0 is the energy of the ground state Ψ_0. Notice that, in contrast to the IA, the internal dynamics of electrons is herein considered. In the insertion of (27) into expressions (2b) for ρ_E and (8a) and (8b) for $\boldsymbol{j}_i$ and $\boldsymbol{j}_{E,i}$, the term $E_0\Psi$ can be omitted; it is easy to verify that this does not change the value of Ω^2. The resulting expressions are

$$\rho_E(\mathbb{R}, t) = \rho^0\rho^d_E, \tag{28}$$

$$\boldsymbol{j}_i(\mathbb{R}, t) = \rho^0\boldsymbol{j}^d_i + \rho^d\boldsymbol{j}^0_i, \tag{29}$$

$$\boldsymbol{j}_{E,i}(\mathbb{R}, t) = \rho^0\boldsymbol{j}^d_{E,i} + \rho^d_E\boldsymbol{j}^0_i, \tag{30}$$

where $\rho^0 = |\Psi_0|^2$ and $\boldsymbol{j}^0_i$ are, respectively, the density and current in the unperturbed electron system. The latter, if existent, can be safely excluded in further consideration. The variables with the upper index d are defined by the same expressions (2) and (8) where Ψ is replaced by $\mathcal{D}$ and $\mathcal{H}_0$ by $\mathcal{T}$. Further, for the indistinguishable electrons the distortion $\mathcal{D}$ is expressed as a product of identical factors:

$$\mathcal{D}(\mathbb{R}, t) = \prod_i D(\boldsymbol{r}_i, t). \tag{31}$$

We can introduce one-electron densities and current densities in three-dimensional space which are later denoted by the same symbols ρ and $\boldsymbol{j}$, respectively.

Substitution of (28)–(30) into Eqs. (9)–(12) results in the equation for straggling [in Eq. (8b) separately consider the terms with $j = i$ and $i \neq j$, where j is the index of the electron in the sum of kinetic energies (4)]

$$\frac{d\Omega^2}{dt} = \frac{d\Omega^2_0}{dt} + \frac{d\Delta\Omega^2_c}{dt}, \tag{32}$$

where

$$\frac{d\Omega^2_0}{dt} = 2n\int d^3\boldsymbol{r}\,\boldsymbol{\mathcal{E}}(\boldsymbol{r}, t)\boldsymbol{j}^d_E(\boldsymbol{r}, t), \tag{33}$$

$$\frac{d\Delta\Omega^2_c}{dt} = 2n\int d^3\boldsymbol{r}_1 d^3\boldsymbol{r}_2 n[g(\boldsymbol{r}_1, \boldsymbol{r}_2) - 1]\rho^d_E(\boldsymbol{r}_1, t)\frac{d\rho^d_E(\boldsymbol{r}_2, t)}{dt}. \tag{34}$$

Here

$$\frac{d\rho^d_E(\boldsymbol{r}_2, t)}{dt} = \boldsymbol{\mathcal{E}}(\boldsymbol{r}_2, t)\boldsymbol{j}^d(\boldsymbol{r}_2, t) \tag{35}$$

and $g(\boldsymbol{r}_1, \boldsymbol{r}_2)$ is the pair-correlation function,

$$n^2 g(\boldsymbol{r}_1, \boldsymbol{r}_2) = N(N-1)\int d^3\boldsymbol{r}_3\cdots d^3\boldsymbol{r}_N|\Psi_0(\boldsymbol{r}_1, \boldsymbol{r}_2, \ldots, \boldsymbol{r}_N)|^2. \tag{36}$$

In the case of uniform electron gas $g(\boldsymbol{r}_1, \boldsymbol{r}_2) = g(|\boldsymbol{r}_1 - \boldsymbol{r}_2|)$ and used below is the structure factor $S(q)$ defined as the Fourier transformation

$$n[g(|\Delta\boldsymbol{r}|) - 1] = \frac{1}{(2\pi)^3}\int d^3\boldsymbol{q}[S(q) - 1]e^{i\boldsymbol{q}\Delta\boldsymbol{r}}. \tag{37}$$

To satisfy correct boundary conditions, the distortion factor $D(\boldsymbol{s})$, $\boldsymbol{s} = \boldsymbol{r} - \boldsymbol{R}$, is taken in the CDW approach as $D = e^{i\boldsymbol{v}\boldsymbol{s}}\psi^+_{-\boldsymbol{v}}(\boldsymbol{s})$. In the case of Coulomb interaction it is expressed as

$$D(\boldsymbol{s}) = C_0 M(-i\nu, 1, iu) = (F'_0 - iF_0)e^{i(u/2)}, \tag{38}$$

where $M(\alpha, \gamma, z)$ is the confluent hypergeometric function, $C_0 = 2\pi\nu/[\exp(2\pi\nu) - 1]$, and $\nu = -Z_1/v$. With such a choice of sign, $\nu > 0$ corresponds to negatively charged projectiles, the repulsive projectile-electron interaction. The variable u is the parabolic coordinate $u = vs + \boldsymbol{v}\boldsymbol{s}$. In the second form in (38), D is expressed through the function $F_0 = F_0(\nu, u/2)$, the Coulomb scattering wave, and the prime indicates the derivative with respect to the second argument. The function $F_0(\nu, z)$ satisfies the equation

$$F''_0 + \left(1 - \frac{2\nu}{z}\right)F_0 = 0. \tag{39}$$

In these terms, the density and current densities in (33) and (34) are written as

$$\rho_E^d = \frac{\nu v}{s}\left(F_0^2 - F_0'^2\right), \tag{40}$$

$$\boldsymbol{j}^d = \frac{2\nu}{us}F_0^2(v\boldsymbol{s} + s\boldsymbol{v}), \tag{41}$$

$$\boldsymbol{j}_E^d = \frac{\nu v}{2s^2}\left(2F_0F_0'\frac{\boldsymbol{s}}{s} + \left(F_0^2 - F_0'^2\right)(v\boldsymbol{s} + s\boldsymbol{v})\right). \tag{42}$$

These expressions are used in the Appendix to write Eqs. (33) and (34) for Ω_0^2 and $\Delta\Omega_c^2$ in a form appropriate for numerical calculation. It is also shown therein that Eq. (33) for Ω_0^2, the noncorrelation term in straggling, converts to the Bohr formula (1).

Using Eqs. (40)–(42), one can easily derive expressions for the straggling in the perturbation and quasiclassical approaches by just replacing F_0 by the perturbative $F_0 = \sin(u/2)$ or by the WKB solution of Eq. (39), respectively. Though such an analysis is not significant in the present context, one important issue arising in the quasiclassical treatment is worth mentioning. Equation (12) is represented in this approach as

$$\frac{d\langle E^2\rangle}{dt} = 2\pi a^2 v^3 Z_1 n \int_{u_{\min}}^{\infty} \frac{du}{u^2\sqrt{1 - \frac{2a}{u}}}, \tag{43}$$

where $a = -2Z_1/v^2$, $|a|$ is the collision diameter in the Rutherford scattering, and again $a > 0$ for a repulsive interaction. At $a > 0$, the integral over the classically accessible region $u > u_{\min} = 2a$ is convergent and Bohr's result (1) is exactly reproduced. At the same time, in the most interesting case of attractive projectile-electron interaction, $a<0$, $u_{\min}=0$, and the integral in (43) diverges at small u as $\sqrt{1-2a/u}$. However, the flux of $\boldsymbol{j}_{E^2}$ through the surface $u = \text{const}$ also diverges at small u and only accounting for both terms on the right-hand side of (7c) leads to the correct result. Clearly, this issue originates from the fact that the condition, analogous to the Kato cusp condition, is not fulfilled in the classical case. This agrees well with the conclusion made in [11] that, in the description of energy transfer in the projectile-electron collisions, the classical approach fails at small impact parameters $b \lesssim \lambda$, where $\lambda = 1/v$ is the de Broglie wavelength of electron moving with velocity v.

The screening of the projectile field plays an important role at low energies, precisely where the electron correlations are effective (see the next section). In general, results obtained in the distorted-wave approximation are of questionable value if, simultaneously, the interelectron interaction is not taken into account. Considering a collision with an electron, one must take into account the presence of a "third body," all other electrons, and, as shown by Dodd and Greider [16], all interactions in the three-body system must be considered already in the first-order approach. An example of the proper treatment is the RPA description of the electron gas response to external perturbation [2] where a qualitatively different feature, the plasmon excitations, is revealed and the effect of the screening is well illustrated. In the next section, the screening is introduced into Eqs. (33) and (34) by a proper modification of the projectile electric field $\boldsymbol{\mathcal{E}}$.

V. NUMERICAL RESULTS AND DISCUSSION

The results of the preceding section are used herein to describe the effect of electron correlations in the case of a uniform electron gas. The cross term of the kinetic energy operator neglected in the CDW approximation can be estimated as a product of the velocity of a recoiled electron, which is of the order of the projectile velocity, and a typical velocity of unperturbed electrons. Ignoring this term in $\mathcal{H}_0\Psi$ is thus justified if $v \gtrsim v_F$. Notice also that the importance of this term is otherwise diminished when it is averaged over the directions of the velocities. Thus, it is believable that the approach is capable of providing reliable results at $v \gtrsim v_F$ and, moreover, can reveal major trends at lower velocities. This is supported by successful applications of the CDW approach in the description of ion-atom collisions. It has been recognized in this case that the main obstacle for usage of the CDW approximation at lower energies is improper normalization of the wave function of the distorted states of bound electrons [17], a problem that is not significant in the case of a translation-invariant system.

To estimate its effectiveness, the screening of the projectile Coulomb field can be introduced as an additional exponential factor $\exp(-\kappa s/\lambda_{\text{ad}})$ in the potential $V(\boldsymbol{s})$. Here λ_{ad} is the adiabatic distance for the projectile-electron collision $\lambda_{\text{ad}} = v/\omega_p$, where $\omega_p = \sqrt{4\pi n}$ is the plasma frequency. The parameter $\kappa \sim 1$ is to be chosen empirically. Such an isotropic form does not reflect, however, the wakelike pattern of screening of a moving particle. To model this, the screening function is taken further as $\exp(-\kappa u/v\lambda_{\text{ad}})$ and the screening pattern is shaped by the parabolic coordinate curves $u/v = s + x = \text{const}$, with x the coordinate along $\boldsymbol{v}$. The value of $\kappa = 1.5$ is chosen to reproduce the RPA results [18] when an equivalent perturbation approximation $F_0 = \sin(u/2)$ is used in the present method. Figure 1 shows the noncorrelation part of the straggling Ω_0^2 [Eq. (33)] for four values of the conventional parameter $\chi^2 = 1/\pi v_F$ characterizing the electron density, where $v_F = (3\pi^2 n)^{1/3}$ is the Fermi velocity. The RPA results at each χ^2 are presented as the low- and high-velocity asymptotic curves joined at their crossing. Though not perfectly, such a simple model of screening approximately reproduces the general tendency of its variation with χ^2.

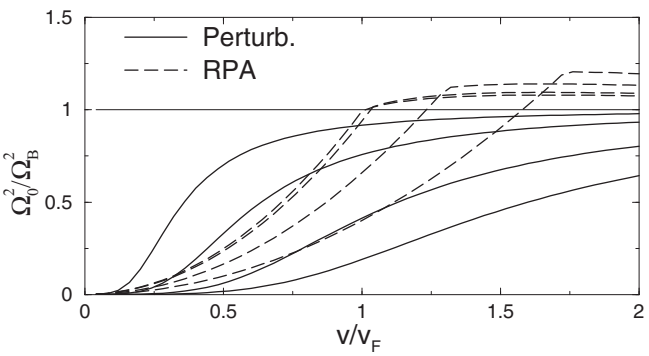

FIG. 1. Perturbation results for the straggling Ω_0^2 at $\chi^2 = 10^{-3}$, 10^{-2}, 0.1, and 0.4 (solid curves from top to bottom, respectively). The dashed lines are the corresponding RPA results.

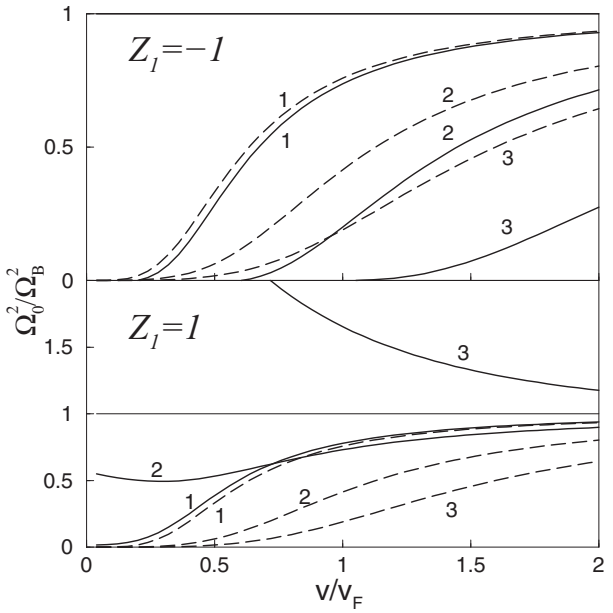

FIG. 2. Results of calculations of Ω_0^2 in CDW approximations (solid curves) compared with the perturbation results for 1, $\chi^2 = 0.01$; 2, $\chi^2 = 0.1$; and 3, $\chi^2 = 0.4$.

In Fig. 2 the perturbation results for $Z_1 = 1$ and $Z_1 = -1$ are shown together with the results obtained in the present CDW approach. At small $\chi^2 = 0.01$, the Fermi velocity is large, $v_F \approx 32$. Consequently, the absolute value of the parameter $\nu = Z_1/v$ is small at almost all velocities v shown; the perturbation approach is thus applicable. An exception is the range $v \lesssim 1$ ($v/v_F \ll 1$) but, as seen in Fig. 2, the field of a projectile moving with such velocities is almost totally screened.

To illustrate the origin of the higher-order corrections seen at larger values of χ^2, Fig. 6 in the Appendix shows the integral in (A1) as a function of the upper limit $u_{\max}$ considered now as variable, the function $U(u_{\max})$ [Eq. (A2)]. It would show the values of Ω_0^2/Ω_B^2 if, instead of the exponential screening, a sharp cutoff of the potential at the equivalent distance $u_{\max} \approx v\lambda_{\rm ad}$ is assumed. It can be seen in the figure that at $\nu < 0$ ($Z_1 > 0$) the attractive interaction results in a concentration of the higher-order effects at small u (close collisions). In the absence of screening, the resulting excess over unity is compensated at larger u and the screening makes this compensation incomplete. At $\nu > 0$ the situation is different; the concentration of effects at the boundary of the classically accessible region $u \approx 4\nu$ is less expressive, the main reason being that the singular behavior of the energy flux $\boldsymbol{j}_E^d$ [Eq. (42)] occurring at the points of classical return is not accompanied in this case by singularity of the projectile field $\boldsymbol{\mathcal{E}}$.

The behavior of $U(u)$ at large u (Fig. 6) has a simple classical explanation. Note first that the contribution of this region to the energy loss is partly due to electrons experiencing close collisions. These recoiled electrons have significant speed and, depending on the sign of Z_1, attractive or repulsive interaction, their energy is additionally decreased or increased in the passage through this region of u. Therefore, weakening

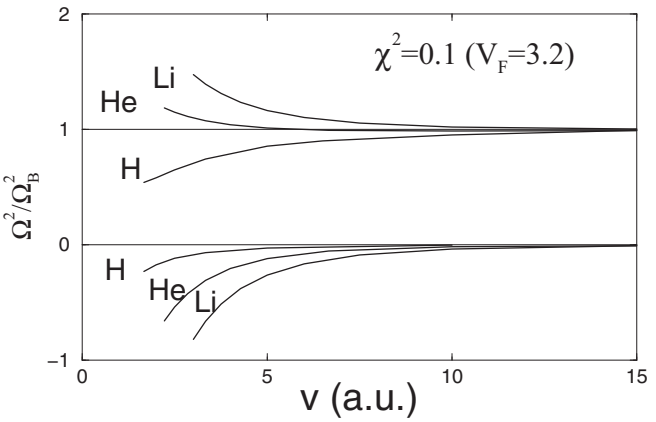

FIG. 3. Velocity dependence of Ω_0^2 (upper curves) and $\Delta\Omega_c^2$ (lower curves).

of the interaction due to the screening results in charge asymmetry of the higher-order correction. The same arguments were used to interpret the origin of the Barkas correction [19] in the mean energy loss [11,20]. Obviously, equivalent results will be obtained in the transport cross-section method [21] if the screening of the projectile field is consistently taken into account. It is worth noting also that the alternative interpretation of the Barkas effect is its association with the electron binding [22], and a special analysis is required to specify which effect is dominating in specific conditions.

At the same time, there is no place here for the even-order correction analogous to the Bloch correction in the stopping cross section [23]. As shown in [11,21], this correction is not related to the screening; the nonlinear corrections in the current density $\boldsymbol{j}(\mathbb{R}, t)$ do not vanish when the integration over all space is fulfilled in (11). In contrast, the integration (12) with the pure Coulomb $\boldsymbol{\mathcal{E}}(\boldsymbol{r}_i, t)$ results in Bohr's straggling and all higher-order effects in $\boldsymbol{j}_E(\mathbb{R}, t)$ are canceled out (see also Ref. [21]).

Calculations of the contribution of the electron correlations $\Delta\Omega_c^2$ were performed using Eqs. (A3), (A7), and (A11). For the structure factor of the electron gas $S(q)$, the analytic approximation [24] of the quantum Monte Carlo data [25] was used. Results for H, He, and Li ions slowing down in the electron gas with $\chi^2 = 0.1$, one of the values characteristic of atomic shells, are shown in Fig. 3. It can be seen in the figure that the value of $\Delta\Omega_c^2$ is of the same order as the magnitude of screening and higher-order effects in Ω_0^2 (deviations from unity of the upper curves). Recall that the CDW approach may be not reliable at $v \lesssim v_F$ and $v_F = 3.2$ in this case. It is believable, however, that the order of magnitude of the corrections is properly reproduced also at such velocities.

Figure 4 shows the results of calculations for He ions, illustrating the contribution of both corrections. Ordinarily, the decrease of Ω^2 at small velocities is attributed to the screening effect alone. However, the present results show that a comparable decrease of the straggling may be produced by electron correlations. At the same time, the higher-order, nonlinear, effects act in the opposite direction. Unfortunately, since Ω_0^2 and $\Delta\Omega_c^2$ are described independently, their summation can result in a nonphysical negative value of Ω^2,

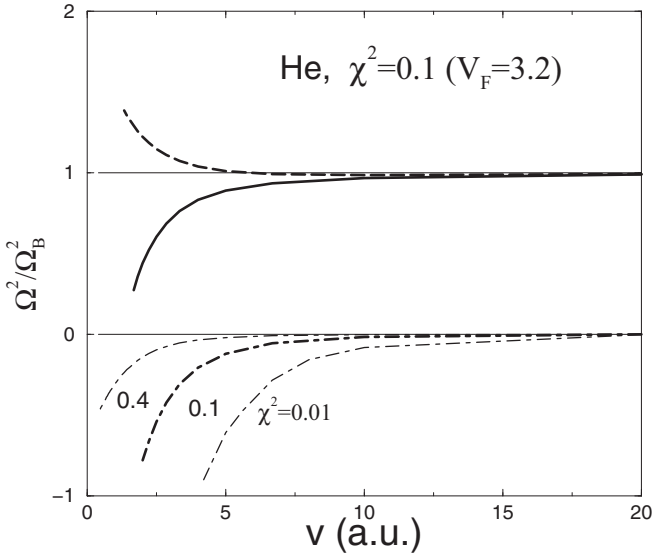

FIG. 4. Total straggling Ω^2 of He ions moving in electron gas with $\chi^2 = 0.1$. The dashed curve on top shows Ω_0^2 and the bold dash-dotted curve on the bottom shows $\Delta\Omega_c^2$. For an explanation of the two other dash-dotted curves see the text.

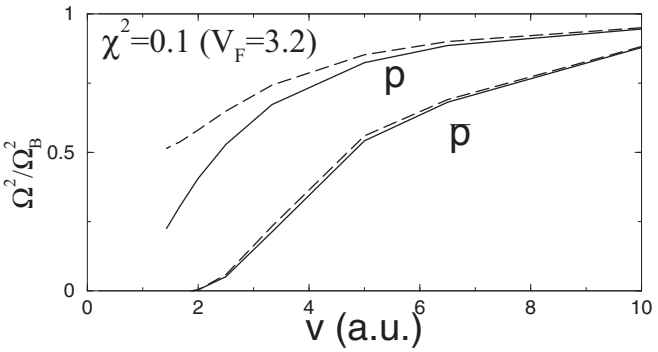

FIG. 5. Comparison of the energy-loss straggling of protons and antiprotons. The dashed curves show Ω_0^2, the straggling in the absence of electron correlations.

as observed at very small velocities. Actually, however, all approximations used lose their applicability at such velocities.

The values of $\Delta\Omega_c^2$ are determined by both the screening and the correlation function $g(r)$. To separately illustrate the effect of correlations, three results for $\Delta\Omega_c^2(v)$ are shown in Fig. 4 (dash-dotted curves). These results are obtained using the same screening function, determined at $\chi^2 = 0.1$, but with different correlation functions. Specifically, the structure factor $S(q)$ was calculated for different densities of electron gas, the values of χ^2 were taken as in Fig. 2. As shown in Fig. 4, the effect of the correlations increases when χ^2 is decreased; this is explained as follows. The factor $n[g(\boldsymbol{r}_1, \boldsymbol{r}_2)-1]$ in the integrand of (34) represents the exchange-correlation hole, the depletion of density of other electrons in the vicinity of one distinct. The volume of the hole is equal to -1, the conservation of the number of electrons, and its width is scaled proportionally to r_s, where r_s is the density parameter, $4\pi r_s^3/3 = 1/n$, $\chi^2 = \alpha r_s$, and $\alpha = (4/9\pi^4)^{1/3} \approx 0.17$. With this hole in the two-particle distribution, the averaging (34) assigns large weights to the products of $\rho_E^d(\boldsymbol{r}_1, t)$ and $d\rho_E^d(\boldsymbol{r}_2, t)/dt$ when r_1 and r_2 are small, less then $\sim r_s$. The weights are approximately proportional to n, hence the observed increase of the absolute value of $\Delta\Omega_c^2$.

The behavior of the electron wave function in the vicinity of the projectile is not changed significantly due to the screening of its field at larger distances and, under the conditions of strong interaction, the defects of the CDW approximation are also insignificant. Thus, these results show that the spatial correlations, an integral feature of a real electron gas, must necessarily be included in theoretical models of straggling of energy loss.

The asymmetry with respect to the sign of the projectile charge is illustrated in Fig. 5, where the straggling of energy loss of protons is compared with that of the antiprotons. The much smaller values of $\Delta\Omega_c^2$ for antiprotons compared to those for protons is easily explained. In the integral (34), the main contribution is provided by the region where all three factors in the integrand have significant values. For the last two factors in the case of protons, this happens at small $\boldsymbol{r}_1$ and $\boldsymbol{r}_2$, where, simultaneously, the pair-correlation function has its minimum. Such a picture is significantly smeared out in the case of repulsive projectile-electron interaction where the close approach of collision partners is not allowed.

Møller *et al.* [26] measured the straggling of protons and antiprotons in Al, Ni, and Au foils but at low energies 1–70 keV where the CDW approach is hardly applicable. In the measurement results, the effects discussed here are strongly obscured by additional fluctuations of energy loss due to inhomogeneity of the target foils. However, at least for one, Al, foil, the straggling of antiprotons is seen to be lower; thus the type of charge sign asymmetry is the same as in Fig. 5. In this paper, the measurement results are compared with calculations carried out in the binary collision approach [27]. Before correcting for the target inhomogeneity, the calculation result shows also the Barkas effect comparable to that predicted in Fig. 5. It is however hardly doubtful that the classical model used in the approach is suitable in these conditions. Really, as it is argued in [11], the classical description of energy loss is not applicable at $v \lesssim 1$. The reason is that any wave packet of an electron with the width in the transverse direction δb spreads during the time of collision $\tau \sim b/v$ to the width $b/v\delta b > 1$ since, clearly, $\delta b/b$ must be small. However, even with $\delta b/b \sim 1$ the wave packet spreads to the size of an atom, and thus the desired picture of the electron moving along a classical trajectory cannot be realized.

VI. SUMMARY

In most approaches, the energy loss of a charged projectile is expressed as a sum of probabilities of excitations of the target electrons weighted with the corresponding energies of transitions. The only alternative used hitherto is calculation of the backreaction of the medium, the retarding force acting on the projectile from the polarized electron cloud [2]. The present paper provides further development of the method where the energy deposition is determined locally at each point of the stopping medium. Provided the perturbed wave

function of electrons is known, at least approximately, this greatly simplifies further analysis.

In Sec. II the same method was used to describe the density of energy squared. The method was applied to describe the energy-loss straggling using two approximations for the perturbed wave function: the IA and CDW approximations. It has been demonstrated that, in contrast to the mean energy loss, the straggling is sensitive to the correlations of projectile collisions with different electrons. Neglecting the interelectron interaction during the collisions, one can consider only pair correlations. It was shown in Sec. III that the treatment of a projectile collision in the impulse approximation turns out to be rather cumbersome. Fortunately, calculations in the CDW approach, which are more reliable in general, are feasible. In contrast to the IA, two features, distortion of the wave function and the initial motion of electrons, are considered in this case independently. Compared to the effect of correlations of collisions with atoms discussed previously [6], the electron correlations, an inherent feature of any multielectron system, modify the statistics of close collisions with electrons which are the main cause of the straggling.

Except for the screening of the projectile field, the straggling at low velocities is modified also due to the higher-order correction over Z_1. This correction originates from the same effect as that responsible for the Barkas correction in the stopping cross section, and its effect is comparable to the effect of electron correlations. For positively charged projectiles, the higher-order and correlation corrections are of opposite signs; they could effectively compensate one another. At $Z_1 < 0$, in contrast, the higher-order correction originating from the distant collisions is still effective, while the effect of electron correlations is less pronounced.

Charge exchange of ions in a medium, not accounted for in the preceding consideration, can effectively contribute to the straggling. The effect is twofold: First, electrons bound to the ion additionally screen the Coulomb field of the projectile nucleus and, second, electron capture and loss events themselves result in energy losses. Provided the dynamics of charge exchange is known, the former effect can be accounted for in the proposed scheme of calculation. On the other hand, this scheme provides also an alternative vision of effects due to the electron captures and losses. Ordinarily, they are believed to result in sharp changes of momentum of the projectile. Here, instead, the effects are to be presented as a specific modification of the current densities $\boldsymbol{j}(\boldsymbol{r}, t)$ and $\boldsymbol{j}_E(\boldsymbol{r}, t)$, both being smooth functions of time. Basically, the jumps in charge state, as if really occurring, do not fit in the picture of a smoothly evolving quantum state of electrons.

To reveal the considered effects in experimental data, a performance of detailed calculations is required where, following the Lindhard-Sharff model [28], the results for a uniform electron gas are to be averaged over the distribution of electron density in an atom. Such work is beyond the scope of the present paper.

Neither of the approximations considered provides a reliable description at low energies. At these energies, the density-functional theory is seen as an attractive alternative. The electron correlations are inherently included in this theory. Runge and Gross [29] developed a nonstationary version of this approach, the time-dependent density-functional theory, which was used already in the description of the mean energy loss [30]. Considering the results of the present paper, the current density-functional theory developed by Dhara and Ghosh [31] seems even more attractive.

ACKNOWLEDGMENT

I am much indebted to P. Sigmund for help received in discussions and for valuable suggestions.

APPENDIX: FORMULAS FOR NUMERICAL EVALUATION OF Ω_0^2 AND $\Delta\Omega_c^2$

Herein the expressions (33) and (34) for the components of straggling Ω_0^2 and $\Delta\Omega_c^2$ are represented in a form facilitating numerical calculations. The integration in these expressions is easier to perform when the parabolic coordinates are used: $u = vs + \boldsymbol{vs}$, $w = vs - \boldsymbol{vs}$ ($\boldsymbol{s} = \boldsymbol{r} - \boldsymbol{R}$), and the azimuthal angle φ. The volume element in these variables is

$$d^3\boldsymbol{s} = \frac{1}{2v^2} s\, du dw d\varphi, \quad s = |\mathbf{s}| = \frac{u+w}{2v}.$$

Let us consider first the case of the nonscreened Coulomb potential of the projectile-electron interaction $V(\boldsymbol{r}, t) = -Z_1/s = \nu v/s$ and $\boldsymbol{\mathcal{E}} = \nu\boldsymbol{vs}/s^3$. Substitution of (42) into (33) gives

$$\left(\frac{d\Omega_0^2}{vdt}\right) = 4\pi Z_1^2 n \int_0^\infty \frac{du}{u^2}\left[2F_0F_0' + u\left(F_0^2 - F_0'^2\right)\right]. \quad \text{(A1)}$$

For the integral on the right-hand side, the indefinite integral is found to be

$$U(u) = F_0^2 + F_0'^2 - \frac{2}{u}F_0F_0' - \frac{4\nu}{u}F_0^2. \quad \text{(A2)}$$

Knowing also that at small u the function $F_0(\nu, u/2) \approx C_0 u/2$ and at large u it behaves as $\sin(u/2 + \sigma)$, where σ is a constant phase [32], we arrive at Bohr's result (1), as expected. Figure 6 illustrates details of the behavior of $U(u)$ for different signs of the projectile charge. To account for the screening, it is necessary to add an additional factor, the screening function, to the integrand in (A1).

In Eq. (34) it is convenient to perform the Fourier transform

$$\frac{d\Delta\Omega_c^2}{dt} = \frac{2n}{(2\pi)^3}\int d^3\boldsymbol{q}[S(q) - 1]\rho_E^d(\boldsymbol{q})\frac{d\rho_E^d(-\boldsymbol{q})}{dt}, \quad \text{(A3)}$$

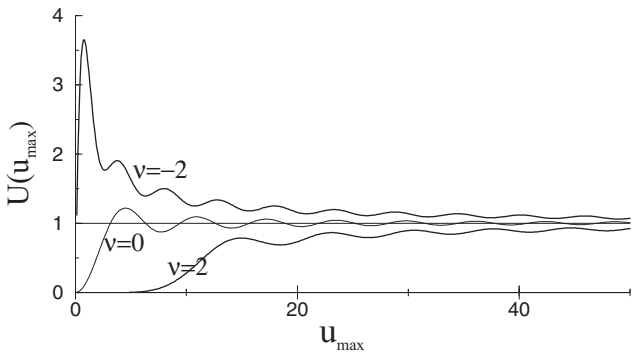

FIG. 6. Integral in (A1) as a function of the upper limit, the function (A2).

where, according to Eqs. (40), (41), and (35),

$$\rho_E^d(\boldsymbol{q}) = \nu v \int \frac{d^3\boldsymbol{s}}{s}\left(F_0^2 - F_0'^2\right)e^{i\boldsymbol{q}\boldsymbol{s}}, \tag{A4}$$

$$\frac{d\rho_E^d(-\boldsymbol{q})}{dt} = 2\nu^2 v \int d^3\boldsymbol{s}\frac{1}{s^3}F_0^2 e^{-i\boldsymbol{q}\boldsymbol{s}}. \tag{A5}$$

The only factor dependent on w and φ in the integrand in (A4) is

$$e^{i\boldsymbol{q}\boldsymbol{r}} = e^{i(k_\parallel(u+w)+2k_\perp\sqrt{uw}\cos\varphi)},$$

where $\boldsymbol{k} = \boldsymbol{q}/2v$ and $k_\parallel$ and $\boldsymbol{k}_\perp$ are, respectively, the longitudinal and transverse components of this vector with respect to $\boldsymbol{v}$. Integration of this factor over φ results in the Bessel function $J_0(2k_\perp\sqrt{uw})$, and then the integral over w is taken as [33]

$$\int_0^\infty dw\, J_0(2\alpha\sqrt{w})e^{-i\beta w} = -\frac{i}{\beta}e^{i(\alpha^2/\beta)}.$$

The result is

$$\rho_E^d(\boldsymbol{q}) = -\frac{i\pi\nu}{vk_\parallel}\int_0^\infty du\left(F_0^2 - F_0'^2\right)e^{i(\alpha+i\epsilon)u}, \tag{A6}$$

where $\alpha = k^2/k_\parallel$ and the positive infinitesimal ϵ is added to ensure convergence of the integral. Finally, after integration by parts with replacement of F_0'' with that from (39), Eq. (A6) is converted to

$$\rho_E^d(\boldsymbol{q}) = -\frac{2i\pi\nu}{vk_\parallel}\left(2\nu - i\alpha^2\frac{\partial}{\partial\alpha}\right)I_0(\nu, \alpha + i\epsilon), \tag{A7}$$

where

$$I_0(\nu, t) = \int_0^\infty \frac{du}{u}F_0^2\left(\nu, \frac{u}{2}\right)e^{itu}. \tag{A8}$$

Using the relation [32]

$$F_0(\nu, z) = C_0 z e^{-iz}M(1 - i\nu, 2, 2iz),$$

this integral is taken using Nordsieck's method [34]

$$I_0(\nu, t) = \frac{C_0^2}{4}[-i(t+1)]^{-1+i\nu}[-i(t-1)]^{-1-i\nu} \times F\left(1 - i\nu, 1 + i\nu; 2; \frac{1}{1-t^2}\right), \tag{A9}$$

where $F(\alpha, \beta; \gamma; z)$ is the hypergeometric function.

To transform (A5) in the same way, we first add one more integration replacing the factor $1/s^3$ in the integrand by

$$\frac{1}{s}\int_0^\lambda \frac{dx}{x^3}e^{-s/x} = \left(\frac{1}{s^3} + \frac{1}{\lambda s^2}\right)e^{-r/\lambda}.$$

At $\lambda = \infty$ this expression gives the desired factor $1/s^3$ and, as can be easily checked, a finite λ corresponds to the screening of the projectile Coulomb field in the form

$$V(\boldsymbol{s}) = \frac{\nu v}{s}e^{-s/\lambda}. \tag{A10}$$

Thus λ defines the value of the screening radius.

The main result of such modification is lowering of the power of s in the denominator of the integrand in (A5), which allows one, after the change of order of integration over x and over $\boldsymbol{s}$, to apply again Nordsieck's method:

$$\frac{d\rho_E^d(-\boldsymbol{q})}{dt} = 8\pi\nu^2 v\int_0^\lambda \frac{dx}{x^2(k_\parallel x + i)}\frac{\partial}{\partial\beta}I_0(\nu, \beta + i\epsilon), \tag{A11}$$

where I_0 is the same integral (A8) and

$$\beta = -\frac{1 + k^2x^2}{x(k_\parallel x + i)}. \tag{A12}$$

Note that this method admits some freedom in choosing the screening function; the exponent in (A10) can be taken as an arbitrary linear combination of u and w.

The advantage of derived Eqs. (A7) and (A11) is that the integration of the oscillating function $F_0(\nu, u/2)$ has been performed analytically. The integral $I_0(\nu, t)$ [Eq. (A9)] is a smooth function of t with the only (integrable) singularity at $t = \pm 1$ [the two factors in front of the hypergeometric function in (A9)]. With $t = \alpha = k^2/k_\parallel$ as in (A7), this corresponds to the condition $q^2 = 2\boldsymbol{v}\boldsymbol{q}$ associated with the Bethe ridge. Note that when taken into account, the screening eliminates this singularity.

[1] N. Bohr, Philos. Mag. **25**, 10 (1913).
[2] J. Lindhard, K. Dan. Vidensk. Selsk. Mat.-Fys. Medd. **28**, No. 8 (1954).
[3] J. Lindhard and A. Winther, K. Dan. Vidensk. Selsk. Mat.-Fys. Medd. **34**, No. 4 (1964).
[4] W. K. Chu, Phys. Rev. A **13**, 2057 (1976).
[5] N. A. Weiss, *A Course in Probability* (Addison-Wesley, Reading, 2005).
[6] P. Sigmund, Phys. Rev. A **14**, 996 (1976).
[7] V. I. Meshakin, J. Phys. B **33**, L303 (2000).
[8] R. G. Newton, *Scattering Theory of Waves and Particles* (Springer, New York, 1982).
[9] S. Borbély, X.-M. Tong, S. Nagele, J. Feist, I. Březinová, F. Lackner, L. Nagy, K. Tökési, and J. Burgdörfer, Phys. Rev. A **98**, 012707 (2018).
[10] D. Cox, *Renewal Theory* (Methuen, London, 1970).
[11] V. A. Khodyrev, J. Phys. B **33**, 5045 (2000).
[12] V. A. Khodyrev, Phys. Scr. **64**, 53 (2001).
[13] L. D. Landau and E. M. Lifshitz, *Quantum Mechanics* (Pergamon Press, Oxford, 1977).
[14] T. Kato, Commun. Pure Appl. Math. **10**, 151 (1957).
[15] I. M. Cheshire, Proc. Phys. Soc. **84**, 89 (1964).
[16] L. R. Dodd and K. R. Greider, Phys. Rev. **146**, 675 (1966).
[17] D. S. F. Crothers, J. Phys. B **15**, 2061 (1982).
[18] E. Bonderup and P. Hvelplund, Phys. Rev. A **4**, 562 (1971).
[19] W. H. Barkas, W. Birnbaum, and F. M. Smith, Phys. Rev. **101**, 778 (1956).
[20] J. Lindhard, Nucl. Instrum. Methods **132**, 1 (1976).
[21] J. Lindhard and A. H. Sørensen, Phys. Rev. A **53**, 2443 (1996).
[22] P. Sigmund and A. Schinner, Eur. Phys. J. D **23**, 201 (2003).

[23] F. Bloch, Ann. Phys. (Leipzig) **408**, 285 (1933).
[24] P. Gori-Giorgi, F. Sacchetti, and G. B. Bachelet, Phys. Rev. B **61**, 7353 (2000).
[25] G. Ortiz, M. Harris, and P. Ballone, Phys. Rev. Lett. **82**, 5317 (1999).
[26] S. P. Møller, A. Csete, T. Ichioka, H. Knudsen, H.-P. E. Kristiansen, U. I. Uggerhøj, H. H. Andersen, P. Sigmund, and A. Schinner, Eur. Phys. J. D **46**, 89 (2008).
[27] P. Sigmund and A. Schinner, Eur. Phys. J. D **12**, 425 (2000).
[28] J. Lindhard and M. Sharff, K. Dan. Vidensk. Selsk. Mat.-Fys. Medd. **27**, No. 15 (1953).
[29] E. Runge and E. K. U. Gross, Phys. Rev. Lett. **52**, 997 (1984).
[30] J. M. Pruneda, D. Sánchez-Portal, A. Arnau, J. I. Juaristi, and E. Artacho, Phys. Rev. Lett. **99**, 235501 (2007).
[31] A. K. Dhara and S. K. Ghosh, Phys. Rev. A **35**, 442 (1987).
[32] *Handbook of Mathematical Functions*, edited by M. Abramowitz and I. A. Stegun (Dover, New York, 1972).
[33] I. S. Gradshteyn and I. M. Ryzhik, in *Table of Integrals, Series, and Products*, 7th ed., edited by A. Jeffrey and D. Zwillinger (Academic Press, San Diego, 2007).
[34] A. Nordsieck, Phys. Rev. **93**, 785 (1954).